MEASURING THE ENERGY HANDLING CAPABILITY OF METAL OXIDE VARISTORS

M.M.R. Ahmed G.A. Putrus L. Ran R. Penlington

University of Northumbria, at Newcastle, UK

Abstract

Metal oxide varistors are widely used in many power electronics circuits to protect against transient over voltages. Certain applications are very demanding on the energy handling capability of the varistors. This paper gives an overview of the failure modes of ZnO varistors and investigates their characteristics when subjected to repetitive current pulses. It describes the puncture failure mode caused by melting of a region in the varistor of local current concentration. Experimental tests are performed to evaluate the puncture energy using an infrared imaging camera. A relationship between the energy absorption and the varistor maximum surface temperature is obtained. It is shown that the destructive energy depends strongly on the uniformity of the varistor; the more uniform, the higher the energy handling capability. The paper also presents the results of nondestructive tests using a scanning acoustic microscope to evaluate the uniformity of the varistor.

Keywords: varistors, infrared imaging camera, energy

INTRODUCTION

Metal oxide varistors (MOV) are highly nonohmic ceramic devices with current-voltage characteristics similar to those of back-to-back Zener diodes but with higher energy handling capability [1]. The voltage-current characteristics of the MOV can be divided into three regions, as shown in Figure 1. At low voltages, in the region known as the pre-switched region, only leakage current occurs. With intermediate voltages in the switched region, the characteristics are generally described by the equation:

$$I = K V^{a}$$

where K and a are parametric constants.

At higher voltages in the up turn region, the varistor current is determined by the resistivity of the ZnO grains [2].

The basic function of ceramic varistors is to protect electronic devices and electrical circuits against voltage surges, such as those generated by lightning strikes and circuit switching transient. Some applications including fault current limiters [3] and active filters [4], require the varistors to absorb continuous repetitive pulses of short duration over a sustained period of time, say 1 second. Therefore, it is necessary to study the energy handling capability of the commercial varistors under these conditions. The research presented in this paper is a step in this direction. In this paper, the energy absorption capability of ZnO varistors is first analysed. Experimental tests on samples of different diameters and thickness are performed to measure the energy handling capability with continuous repetitive pulses. The puncture mechanism caused by current concentration is analysed and discussed.

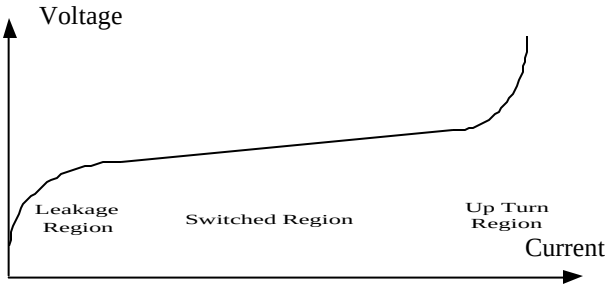

Figure 1 Varistor characteristics

ENERGY HANDLING CAPABILITY OF ZnO VARISTORS

Energy handling capability can be defined as the amount of energy that the varistor can absorb before it fails. Thermodynamically, the energy per unit volume that an ideal varistor is capable of absorbing is determined by the temperature rise due to the energy absorption, which is a function of its density and specific heat [5,6].

$$J_{\max} = r \cdot C_p \cdot (T_2 - T_1) \ \text{J/cm}^3$$

where r = density, g/cm^3

C_p = specific heat, J/g ^{o}C

$T_2 - T_1$ = temperatue rise, ^{o}C

This theoretical relationship assumes that all of the heat generated is absorbed by the varistor and that none is dissipated to the environment. For the MOV, $C_p \approx 0.89$ J/g ^{o}C at 25 ^{o}C and $C_p \approx 1.0$ J/g ^{o}C at 130 ^{o}C. The theoretical density is 5.60 g/cm^3. Hence the volumeteric specific heats are 4.98 and 5.60 J/cm^3 ^{o}C, at the above two temperatures, respectively. Thus, a 100^{o}C temperature rise corresponds to about 500 J/cm^3. The specified energy levels of practical MOV's fall between 200 and 250 J/cm^3.

According to the above, it is obvious that the theoretical energy handling capability of an ideal varistor is directly proportional to its volume.

For MOV to operate without failure or degradation, it must quickly dissipate the absorbed energy and return to its pre-pulse design ambient temperature. The duration of operation, its frequency of occurrence, the geometry of the device, and the operating environment determine the rate of heat dissipation.

In practice, the energy dissipated in the varistor is limited to avoid several types of failures: puncture mode failure, pulse-induced fracture and long term degradation in electrical properties [7,8,9].

The puncture mode failure occurs as a consequence of current localisation and the associated joule heating that leads to a hole being melted through the varistor and shorting the electrodes. The effects of microstructure inhomogenities, such as variation in grain boundary potential and grain size, have been explored using computer modelling. It has been shown that the microstructure inhomogenities can lead to puncture mode failure [9].

The second mode of failure is the mechanical fracture of the varistor when subjected to extremely large but short time pulses. It has been shown that the fracture failure mode occurs with short pulses and the puncture mode with slightly longer pulses [10].

The microstructure nonuniformity of a varistor and its effects on the energy absorption capability have been analysed [10]. The nonuniformity of the current distribution was examined by measuring the current distribution using dot electrodes distributed on the top surface of the varistor. Measurements were taken while the varistor was subjected to currents of different wave shapes and periods.

In this paper, two methods to measure the structure nonuniformity of ZnO varistors are analysed: (a) ultrasonic wave detection and (b) monitoring of the temperature distribution using an infrared radiation thermal-camera.

EXPERIMENTAL SET UP

The objective of the tests is to define the maximum number of repetitive current pulses that the varistor can conduct without failure or damage. The current pulses through the varistor are set to be of fixed amplitude, waveshape and frequency. The varistor temperature is monitored during operation from a few milliseconds up to a few seconds. The use of thermocouple was ruled out as their response is relatively slow and heat distributions are difficult to measure. An infrared imaging system was used to measure the temperature distribution on the varistor surface. The thermal imaging system consists of a scanner, an infrared detector, a computer-based processor, a display device and output instruments (monitor and printer) [11]. Figure 2 shows a schematic diagram of the experimental set up.

Power circuit. Figure 3 shows the power circuit which, produces the current pulses to be injected in the varistor under test. The circuit consists of a d.c. supply (V1), an IGBT, a freewheeling diode (D1 to protect the IGBT from reverse voltage), a snubber circuit (R1, C1 and D2 to protect IGBT from high dv/dt), the test varistor (V) and an RL load bank. Figure 4 shows the experimental set up where the power circuit components are assembled on one board in order to minimise the stray inductance.

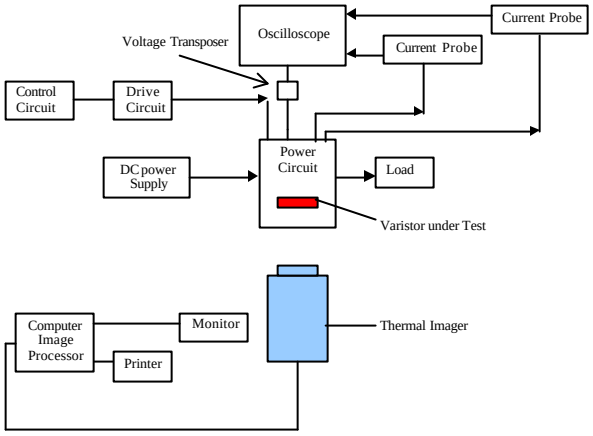

Figure 2 The test system set up

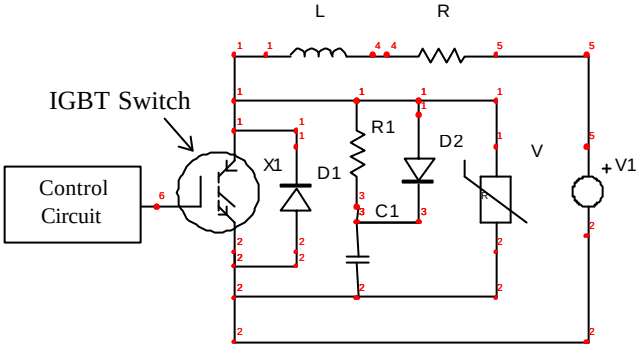

Figure 3 A schematic diagram of the power circuit

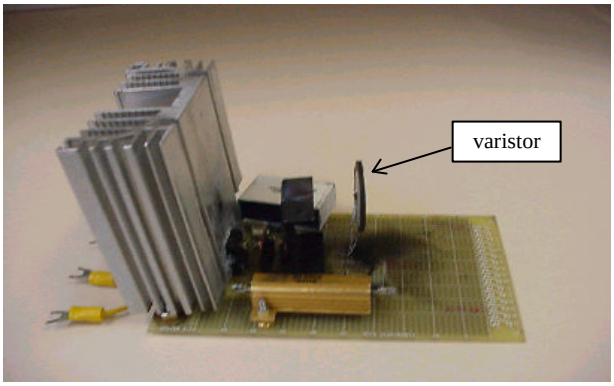

Figure 4 The power circuit lay out

Test varistors: Tests were carried out on samples from two manufacturers with specifications as given in Table-1.

Table-1 Specifications of test varistors

Specification	Product A	Product B
Diameter	36 mm	53 mm
Thickness	2 mm	3.56 mm
Clamping voltage	560 V	650 V
Energy rating	170 J	880 J

Test procedure. Normally, the IGBT is kept in the off state and the supply voltage (less than the varistor clamping voltage) appears across the varistor. When the IGBT is turned on, current starts to flow through the circuit and energy is stored in the load inductance. When the IGBT is now turned off, the inductor tries to maintain the flow of current, as the current through an inductor cannot change abruptly. Consequently, a high voltage across the IGBT and varistor is produced which drives current through the varistor (initially equal to the operating load current ≈20A). The varistor current then decays toward zero exponentially with time. Within each switching cycle, the IGBT is turned on for a period of 540 µs and is then turned off for another period of 540 µs. The switching operation continues for a controllable duration, up to a few seconds.

TEST RESULTS

Thermal images obtained at regular time intervals present a dynamic record of the thermal condition of the varistor. Figure 5 gives a group of thermal images for the 36 mm varistor recorded at an interval of 80 ms for a total recording time of 480 ms. Recording started before IGBT operation which lasted for about 200 ms. The first image in Figure 5 shows the varistor still at room temperature. During the first 240 ms (images 2, 3 and 4), the varistor temperature increased rapidly to more than 127°C at the hottest spot. Images 5 and 6 describe the temperature distribution after the switching operation had stopped. The percentage hot area became larger indicating heat being conducted from the hotter parts to a wider area. The images in Figure 5 show heat localisation with the hottest spot being to the right edge of the disc. The temperature there was higher than 127°C. In contrast, the coldest part of the varistor surface was in the region of 30°C. Such a large difference due to current localisation results in poor utilisation of the varistor volume.

Similar tests were carried out on a 53 mm varistor. Figure 6 shows the measured waveforms for the varistor voltage and current. Figure 7 gives a group of thermal images of the varistor recorded at an interval of 80 ms over a period of 480 ms. Continuous repetitive pulses were applied to the varistor for 400 ms. It is clear from the images shown that heat distribution is more uniform than the previous varistor (36 mm). A relatively mild current concentration spot was identified near the centre of the disc. Heat was evenly dissipated in all directions.

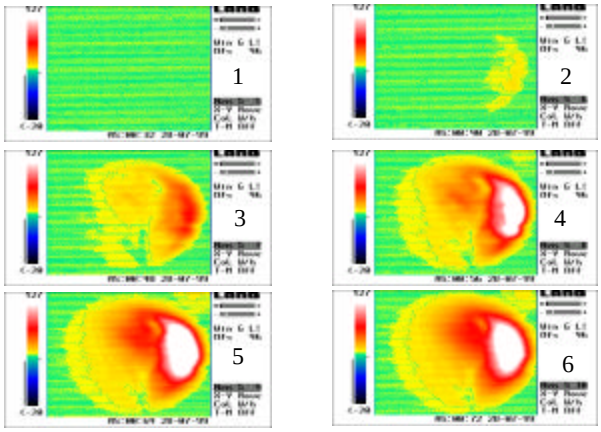

Figure 5 Temperature distribution of product A

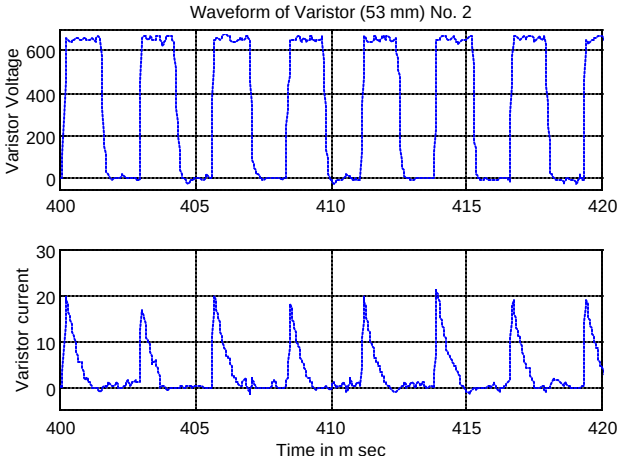

Figure 6 Voltage and current of the product B

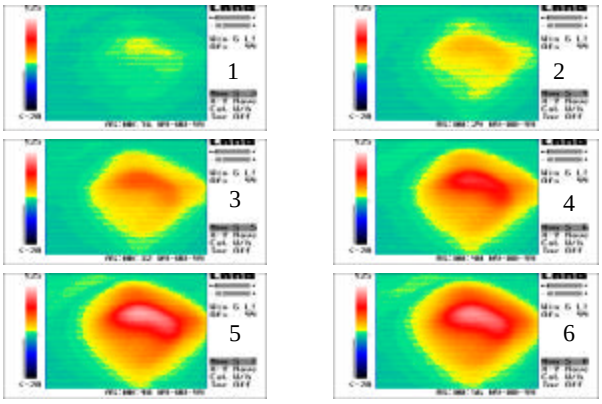

Figure 7 Temperature distribution of product B

MAXIMUM ENERGY HANDLING CAPABILITY OF THE VARISTOR

In order to define the maximum continuous energy that a varistor can absorb without any damage, several tests were performed on three more samples of the 53 mm type varistor. For each sample, thermal images before, during and after the switching operation were recorded. Operation time was varied to change the energy absorbed by the varistor. In each case, the maximum surface temperature of the varistor was monitored. Figure 8 shows, for the three samples, the relationship between the maximum temperature (Tmax) and the switching operation time. Figure 9 shows the relationship between the energy absorption of the varistors (calculated as $\int vidt$) and operation time.

The relationship between varistor temperature versus input energy is derived from Figures 8 and 9 and is shown in Figure 10. In all these tests, the maximum surface temperature of the varistors was raised to about 200°C without causing any damage. Comparing with the specification in Table 1, it is shown that the varistor maximum temperature remains under 200°C even when the total energy absorbed is about twice the "maximum energy absorption", 880 J. It is clear that the varistor can operate with continuous repetitive pulses safely as long as its thermal stability point is not reached. This is because the off periods in the pluses allow some heat to dissipate across the surface of the varistor.

After such tests, the switching time was then increased to gradually reach the puncture mode. Figure 11 shows that there are three regions. Firstly there is the thermal stability region in which the input energy to the varistor will be proportional to the varistor maximum surface temperature. Secondly, there is the region "out of thermal stability", here a small increase in the input energy leads to large temperature rise. Finally, there is the thermal runaway region where the hot spot temperature increases until local varistor puncture occurs.

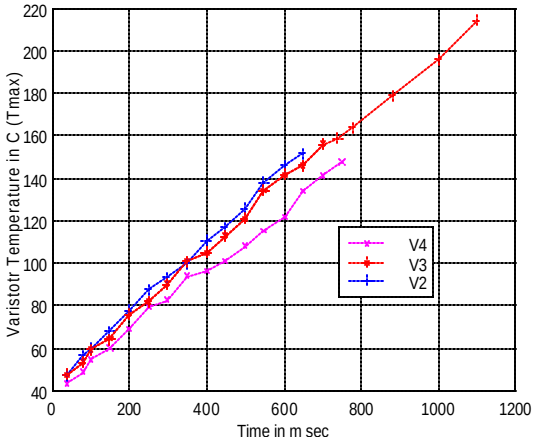

Figure 8 Relationship between varistor temperature and switching time

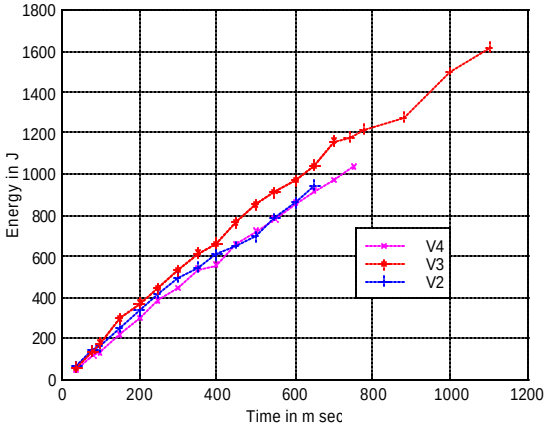

Figure 9 Relationship between input energy and switching time

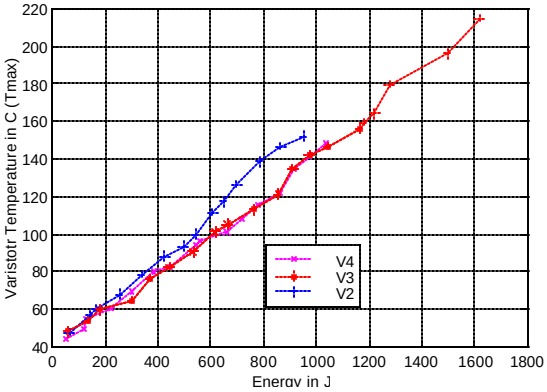

Figure 10 Relationship between varistor temperature and input energy

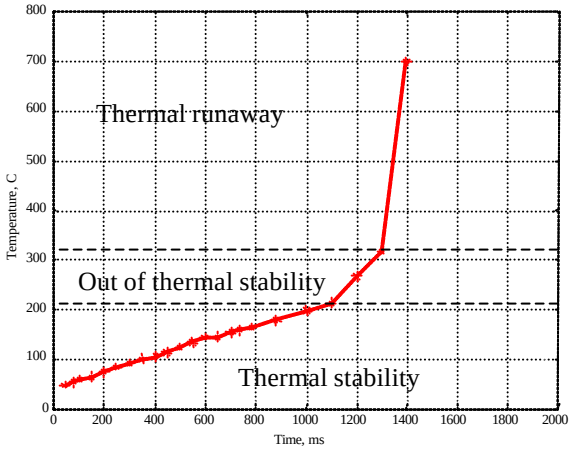

Figure 11 Temperature regions

NONDESTRUCTIVE TEST USING SCANNING ACOUSTIC MICROSCOPE (SAM).

Ultrasonic is commonly used means of nondestructive testing. Pulses of compressional or shear pressure waves at frequencies of 1-100 MHz are generated by a piezoelectric transducer. The pulse passes through the specimen and the reflection is picked up by the same

transducer [12]. The pulse is modified by the path taken and energy is reflected by material discontinuities. The Ultrasonic transducer cannot generally operate in air. Water is therefore used as a transparent medium between the transducer and the specimen to allow ultrasonic energy to transmit into and out of the specimen. Varistors to be tested are placed in trays in an immersion tank and the scanner is positioned to scan under computer control. Figure 12 shows the images of a varistor scanned at different depths. The results obtained for each sample were compared with the corresponding thermal images of the same sample. While a vague correspondence could some times be noticed, no conclusive match could be found. The ultrasonic scanning microscope is more suitable for detecting the cracks or larger porosity.

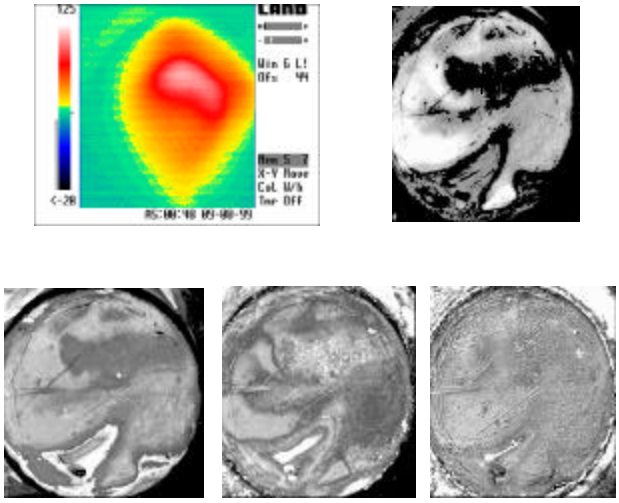

Figure 12 SAM photograph for 53 mm varistor

CONCLUSIONS

The energy handling capability of ZnO varistors has been examined. The experimental results show that:

1. The infrared imaging camera is a useful mean for measuring the energy handling capability, temperature distribution and uniformity of the microstructure of the varistor.
2. The energy handling capability strongly depends on the varistor microstructure uniformity; the more uniform, the higher the energy handling capability.
3. When subjected to continuous repetitive pulses the varistor can handle a total energy higher than the rating usually specified for a single pulse (almost twice).
4. There are three regions before the varistor puncture: the thermal stability region, the out of thermal stability region and the thermal runaway region.
5. The acoustic scanning microscopy does not provide the required resolution for measuring the uniformity of the varistor microstructure. But it can be used to find larger defects.

ACKNOWLEDGEMENTS

The authors would like to thank Northern Electric Distribution Limited and the Regional Center for Electronic Technology (RECET) for their support to this work. Thanks are also due to the Government of Egypt for the scholarship provided to Mr. Ahmed to study at the University of Northumbria, UK.

This paper describes part of a development work, the results of which has been submitted in a patent application.

REFERENCES

1. Lionel M.L., and Herbert R.P., 1986, "Zinc Oxide Varistor A-Review", Ceramic Bulletin, Vol. 65, No. 4, pp. 639-646.
2. Clarke, David R., 1999 "Varistor Ceramics", Journal of the American Ceramic Socity, V82, No. 3, pp. 485-502.
3. Ahmad M. and Putrus, G.A., 1999, "Investigation into Custom Power Technology", UPEC99, Vol. 2, pp. 509-512
4. Moran, L.A.; Pastorini, I.; Dixon, J and Wallace, R., 1999 "A fault protection scheme for series active power filters" IEEE Trans. PE., pp. 928-938
5. Bartkowiak M., and Mahan G.D.,1996, "Energy Handling Capability of ZnO Varistors", J. Appl. Phys., Vol. 79, No. 11, pp. 8629-8633
6. Agens, V. and Clarke D.R.,1997, "Electrical-Impulse–Induced Fracture of Zinc Oxide Varistor Ceramics", J. Am. Ceram. Soc., Vol.80, No. 8, pp. 2086-2092,
7. Mizukoshi A., Ozawa J. and Nakano K., 1983, "Influence of Uniformity on Energy Absorption Capability of Zinc Oxide Elements as Applied in Arresters":, IEEE. Trans. PAS-102, No. 5, pp. 1384-1390.
8. Bartkowiak M., and Mahan G.D., 1999 "Failure Modes and Energy Absorption Capability of ZnO. Varistors", IEEE Trans. PWRD., Vol. 14, No. 1, pp. 152-162.
9. Agens V., and Clarke D. R., 1997 "Microstructural Origin of Current Localisation and Puncture Failure in Varistor Ceramics", J. Appl. Phys., Vol. 81, No. 2, pp. 985-993.
10. Kazuo E., 1984, "Destruction Mechanism of ZnO Varistors due to High Currents", J. Appl. Phys., Vol. 56, No.10, pp. 2948-2955
11. Land Infrared "Land TI 35sm Thermal Imager Operation Instructions", Dronfield UK, 1994.
12. Drinkwater B., 1998 "Sounding out good adhesion", Materials World, pp. 149-151.